



# Cenaero



UCLouvain



## Machine Learning for wall modeling in LES of separating flows

HiFiLeD, 3rd High-Fidelity Industrial LES/DNS Symposium,  
December 14th-16th 2022, Brussels, Belgium

**M. Boxho, M. Rasquin, T. Toulorge, G. Dergham,  
G. Winckelmans and K. Hillewaert**

ULiege, UCLouvain, Cenaero, Safran Tech

Contact: [margaux.boxho@cenaero.be](mailto:margaux.boxho@cenaero.be)

Doc. ref.: 2019030-THSELDP-SAFRAN

RANS frequently fails at **off-design conditions** due to its inherent modeling assumptions.

LES reduces the **modeling assumptions** but remains costly at large Reynolds numbers.

**Wall-models** reduces the computational cost by modeling the near-wall energetic scales.

RANS frequently fails at **off-design conditions** due to its inherent modeling assumptions.

LES reduces the **modeling assumptions** but remains costly at large Reynolds numbers.

**Wall-models** reduces the computational cost by modeling the near-wall energetic scales.

Simulations of turbomachines to compute the **operating points** of the engine.

Calibration of the wall models using **neural networks** with **wrLES** on basic and academic test cases and blades.

In turbomachines, transitional flows are frequently encountered, such as laminar **separation bubbles**.

RANS frequently fails at **off-design conditions** due to its inherent modeling assumptions.

LES reduces the **modeling assumptions** but remains costly at large Reynolds numbers.

**Wall-models** reduces the computational cost by modeling the near-wall energetic scales.

Feed lower-fidelity models on larger components (wmLES)

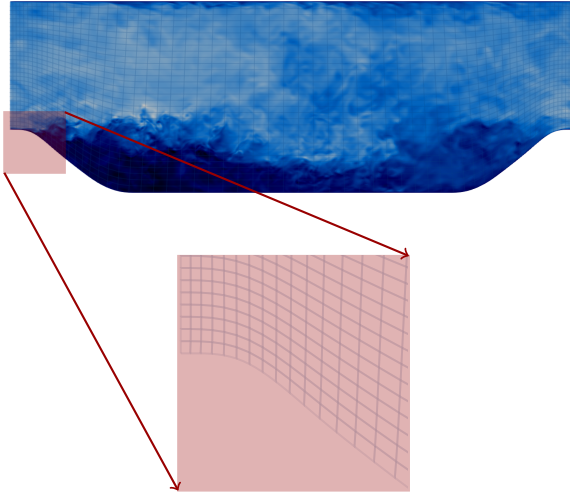
Simulations of turbomachines to compute the **operating points** of the engine.

Calibration of the wall models using **neural networks** with **wrLES** on basic and academic test cases and blades.

In turbomachines, transitional flows are frequently encountered, such as laminar **separation bubbles**.

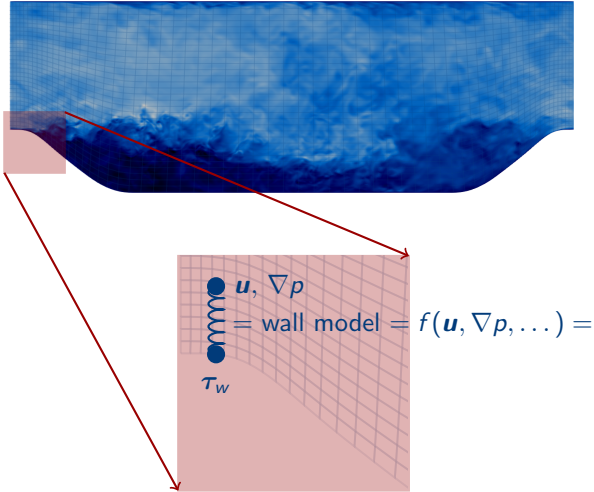
Increasing fidelity on sub-components (wrLES,DNS)

# Wall modeled LES with neural networks

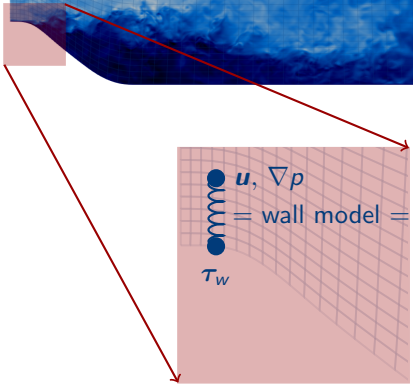
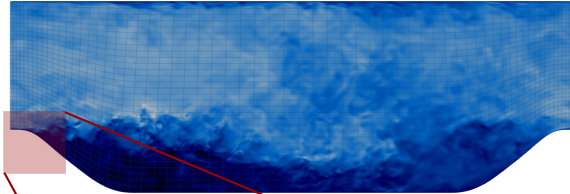


PROD-F-015-02

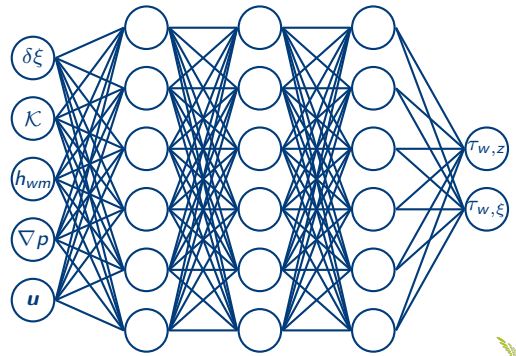
# Wall modeled LES with neural networks



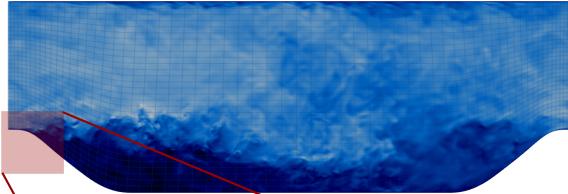
# Wall modeled LES with neural networks



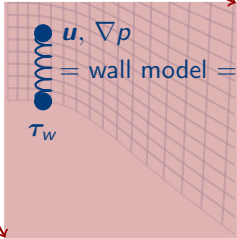
$$\text{wall model} = f(\mathbf{u}, \nabla p, \dots) =$$



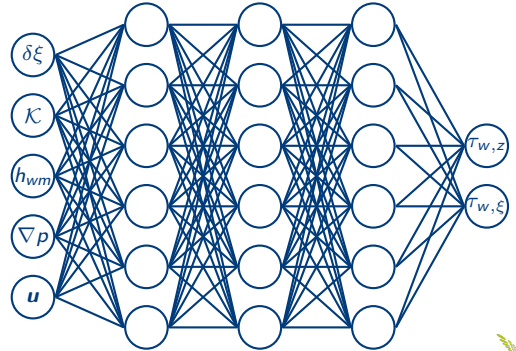
# Wall modeled LES with neural networks



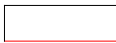
**Problem definition** Finding a complex and dynamic relation between instantaneous fields, geometrical parameters, and the wall-parallel components of the wall shear stress



$$= \text{wall model} = f(\mathbf{u}, \nabla p, \dots) =$$

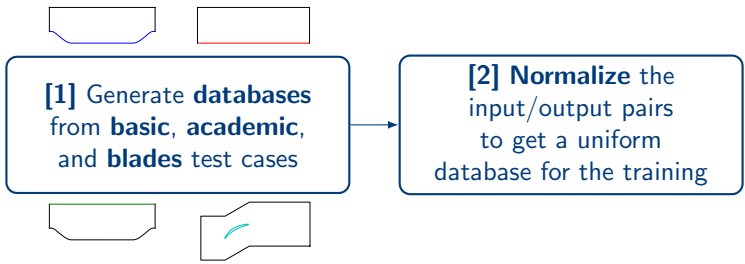


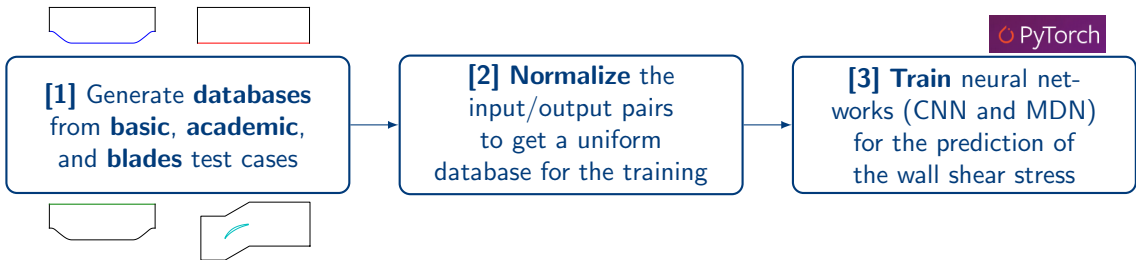


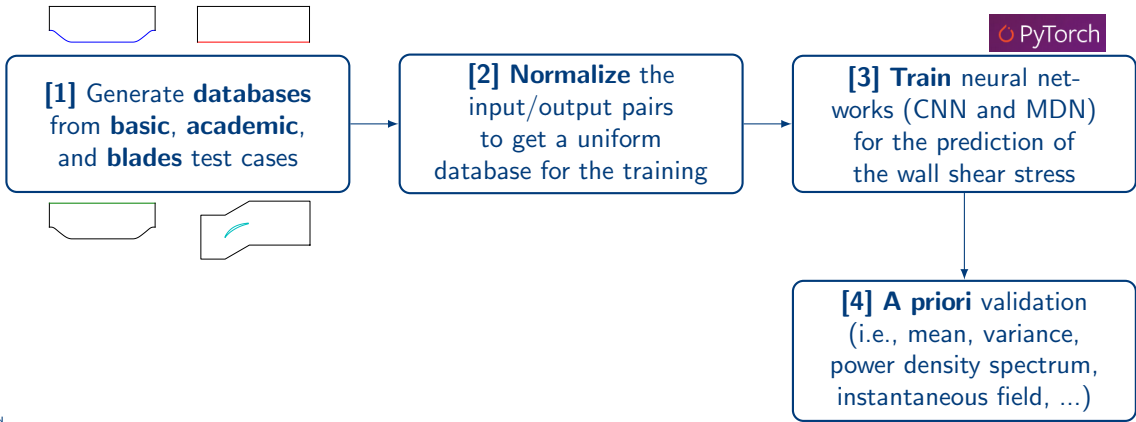


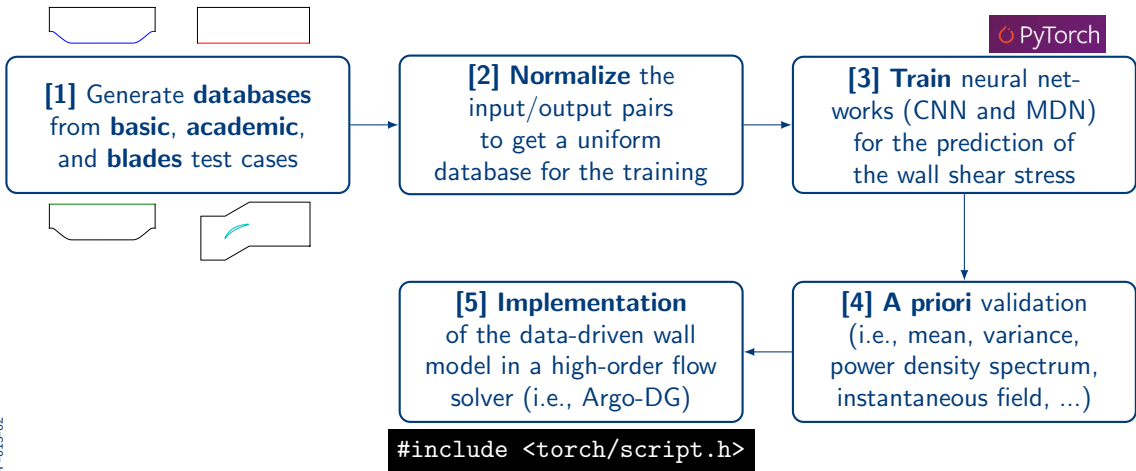
[1] Generate **databases**  
from **basic**, **academic**,  
and **blades** test cases



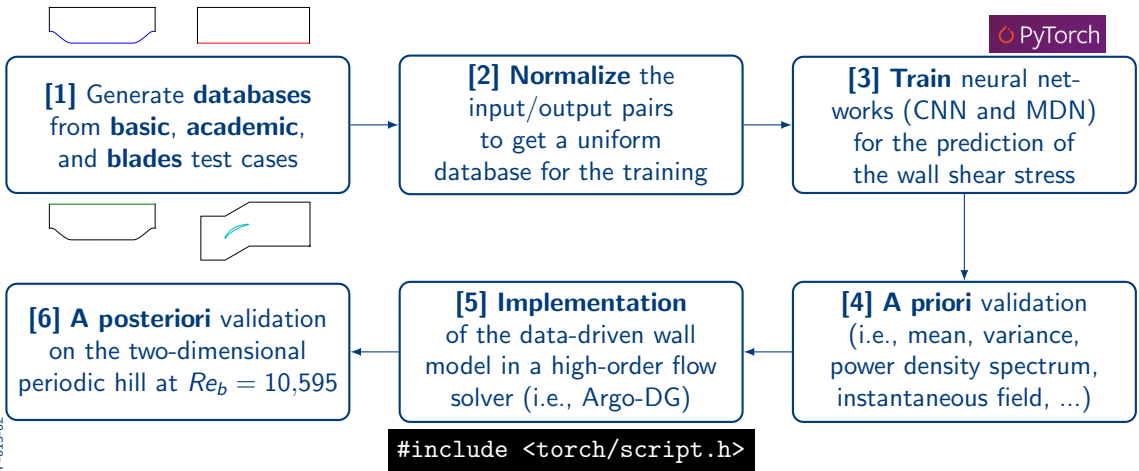






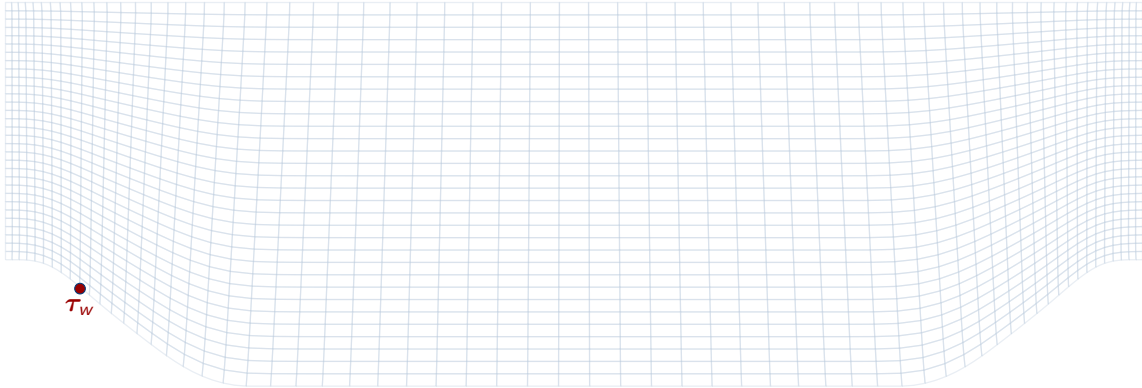


PROD-F-015-02

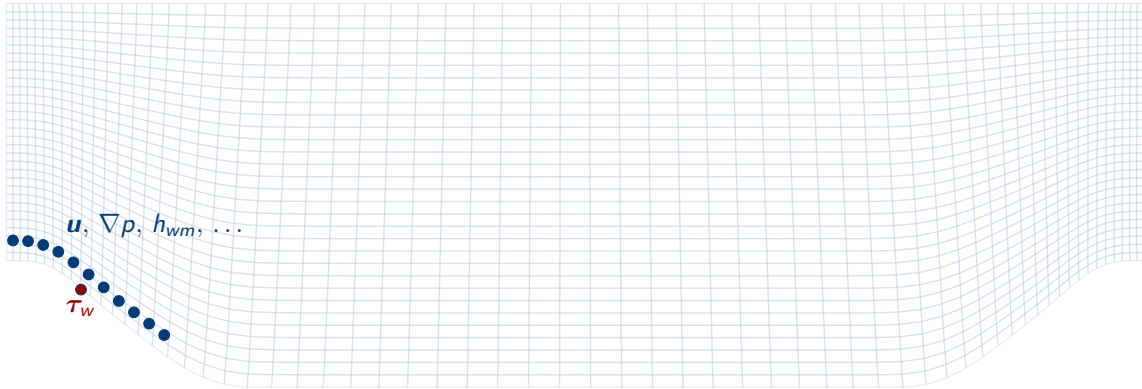


PROD-F-015-02

# Where is the data extracted?

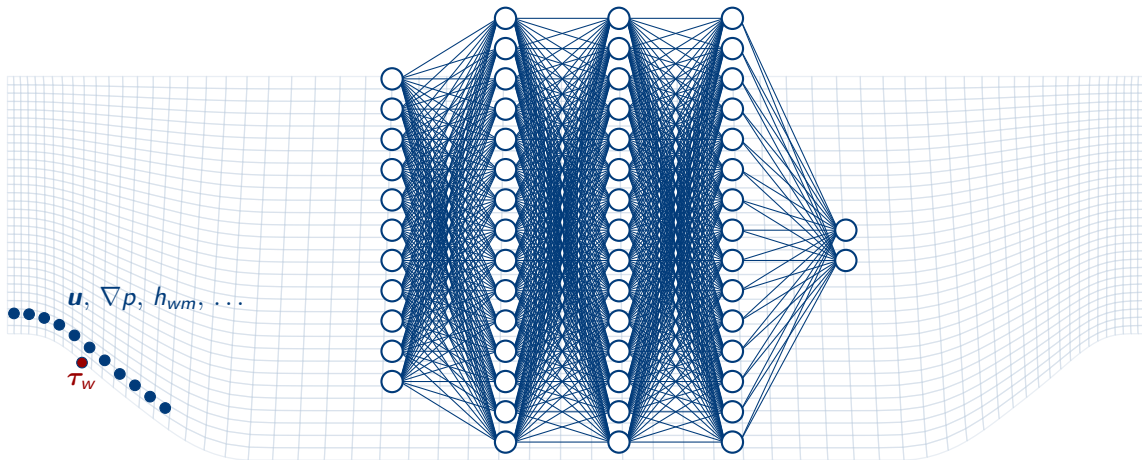


# Where is the data extracted?



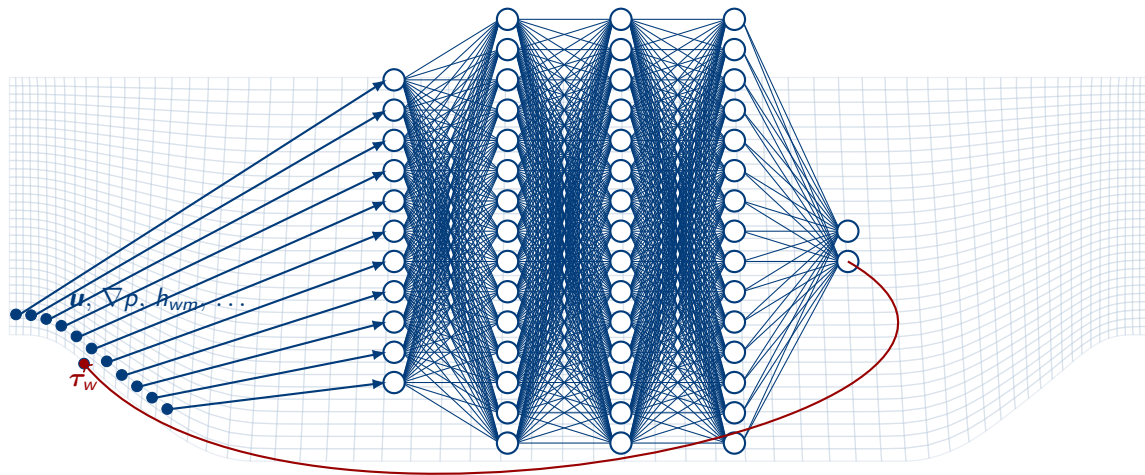


# Where is the data extracted?



## Where is the data extracted?

The input size is based on the analysis of space-time correlations<sup>1</sup>



[1] Boxho, M. et al.: Analysis of space-time correlations to support the development of wall-modeled LES. Flow, Turbulence and Combustion, 2022.

# Normalization of the input/output pairs

The **inputs** are normalized as,

$$\mathbf{u}^* = \frac{\mathbf{u}}{u_{\nu,p}}$$

$$(\nabla p)^* = \frac{h_{wm}}{(\rho u_{\nu,p}^2)} \nabla p$$

$$h_{wm}^* = \ln \left( \frac{h_{wm}}{y_{\nu,p}} \right)$$

$$(\delta \xi)^* = \frac{\delta \xi}{y_{\nu,p}}$$

# Normalization of the input/output pairs

The **inputs** are normalized as,

$$\mathbf{u}^* = \frac{\mathbf{u}}{u_{\nu,p}}$$

$$(\nabla p)^* = \frac{h_{wm}}{(\rho u_{\nu,p}^2)} \nabla p$$

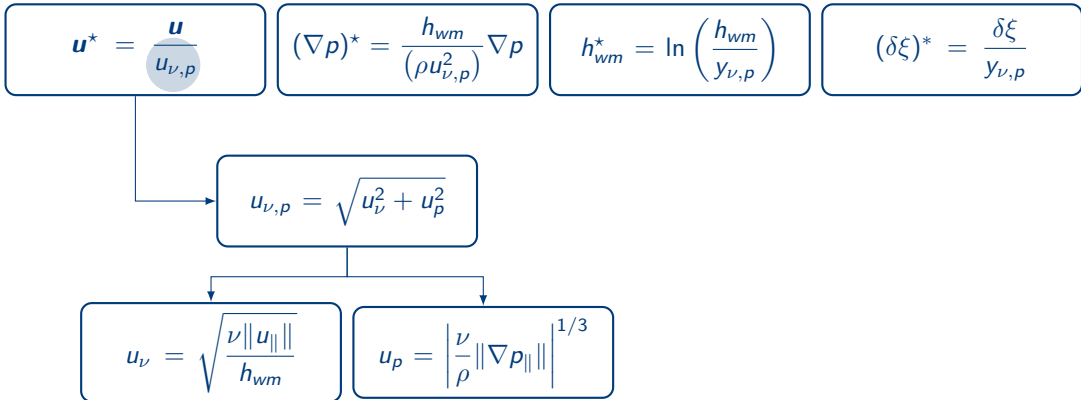
$$h_{wm}^* = \ln \left( \frac{h_{wm}}{y_{\nu,p}} \right)$$

$$(\delta \xi)^* = \frac{\delta \xi}{y_{\nu,p}}$$


$$u_{\nu,p} = \sqrt{u_{\nu}^2 + u_p^2}$$

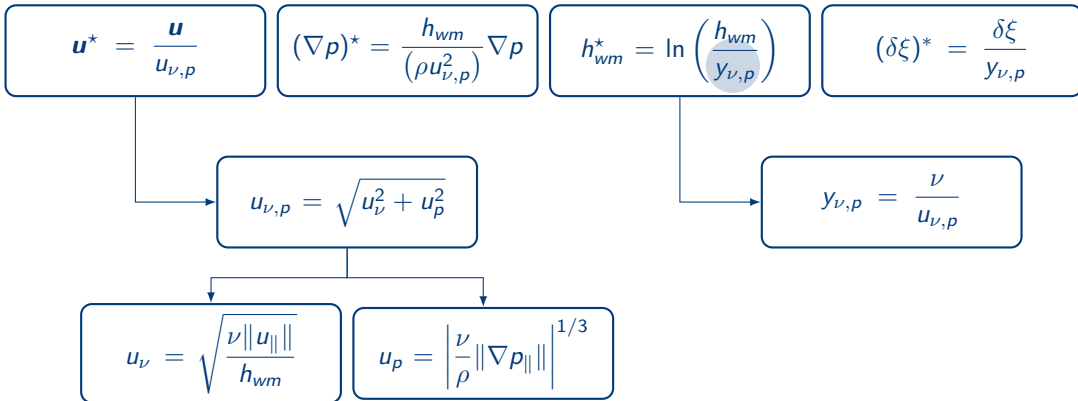
# Normalization of the input/output pairs

The **inputs** are normalized as,



# Normalization of the input/output pairs

The **inputs** are normalized as,



# Normalization of the input/output pairs

The **inputs** are normalized as,

$$\mathbf{u}^* = \frac{\mathbf{u}}{u_{\nu,p}}$$

$$(\nabla p)^* = \frac{h_{wm}}{(\rho u_{\nu,p}^2)} \nabla p$$

$$h_{wm}^* = \ln \left( \frac{h_{wm}}{y_{\nu,p}} \right)$$

$$(\delta \xi)^* = \frac{\delta \xi}{y_{\nu,p}}$$

$$u_{\nu,p} = \sqrt{u_\nu^2 + u_p^2}$$

$$u_\nu = \sqrt{\frac{\nu \|u_{\parallel}\|}{h_{wm}}}$$

$$u_p = \left| \frac{\nu}{\rho} \|\nabla p_{\parallel}\| \right|^{1/3}$$

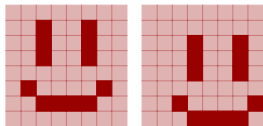
$$y_{\nu,p} = \frac{\nu}{u_{\nu,p}}$$

The **outputs** are normalized as,

$$\tau_w^* = \frac{\tau_w}{\frac{1}{2} \rho \langle u_{\nu,p}^2 \rangle_{\xi,z}}$$

## Convolutional neural network (CNN)

Invariant to **translation**



Prop.

## Mixture Density Network (MDN)

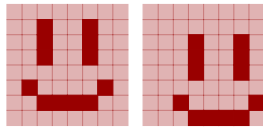
Produces a **distribution** as a linear combination of Gaussian distribution

$$p(y|\mathbf{x}) = \sum_{k=1}^K \pi_k \mathcal{N}(y; \mu_k, \sigma_k^2)$$



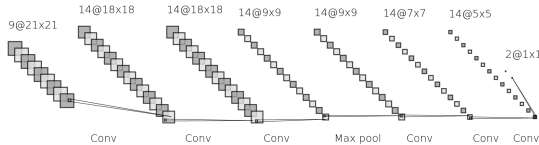
## Convolutional neural network (CNN)

Invariant to **translation**



Prop.

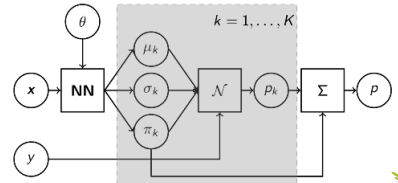
Archit.



## Mixture Density Network (MDN)

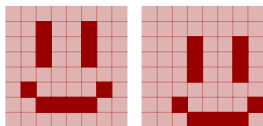
Produces a **distribution** as a linear combination of Gaussian distribution

$$p(y|\mathbf{x}) = \sum_{k=1}^K \pi_k \mathcal{N}(y; \mu_k, \sigma_k^2)$$



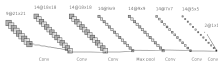
## Convolutional neural network (CNN)

Invariant to **translation**



Prop.

Archit.

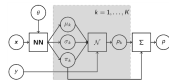


$$\arg \min_{\theta} \sum_{\mathbf{x}_i, y_i \in \mathcal{d}} (y_i - \hat{y}_i)^2$$

## Mixture Density Network (MDN)

Produces a **distribution** as a linear combination of Gaussian distribution

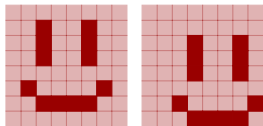
$$p(y|\mathbf{x}) = \sum_{k=1}^K \pi_k \mathcal{N}(y; \mu_k, \sigma_k^2)$$



$$\arg \min_{\theta} \sum_{\mathbf{x}_i, y_i \in \mathcal{d}} \frac{(y_i - \mu(\mathbf{x}_i))^2}{2\sigma(\mathbf{x}_i)} + \log(\sigma(\mathbf{x}_i)) + C$$

## Convolutional neural network (CNN)

Invariant to **translation**



Prop.

Archit.

Obj.  
fun.

$$\arg \min_{\theta} \sum_{x_i, y_i \in \mathcal{d}} (y_i - \hat{y}_i)^2$$

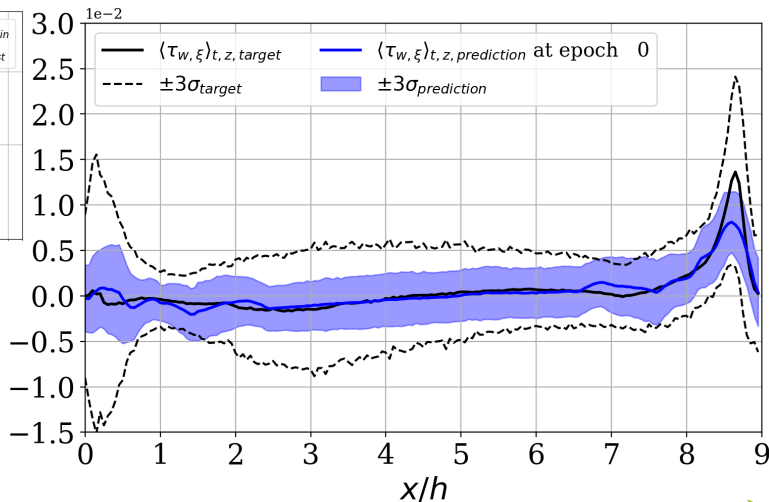
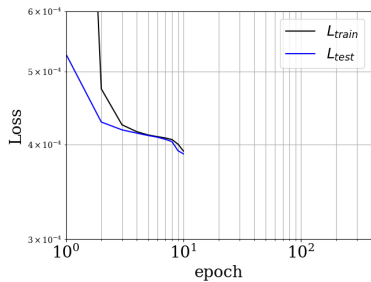
## Mixture Density Network (MDN)

Produces a **distribution** as a linear combination of Gaussian distribution

The prediction is obtained from a **sampling** of the generated distribution.

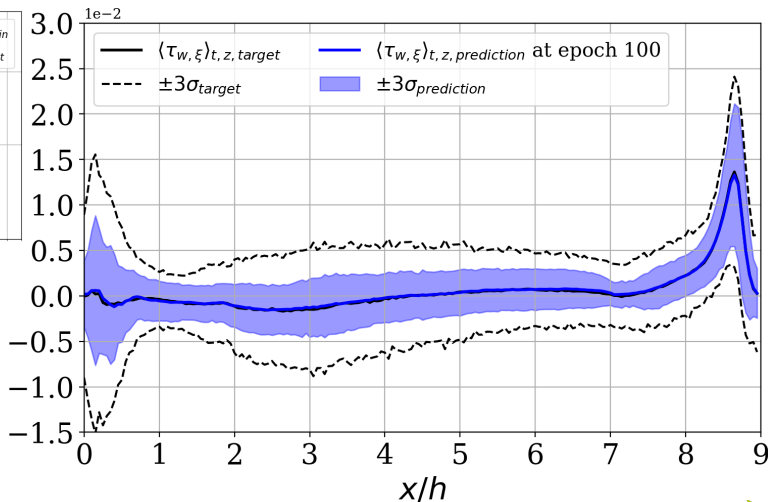
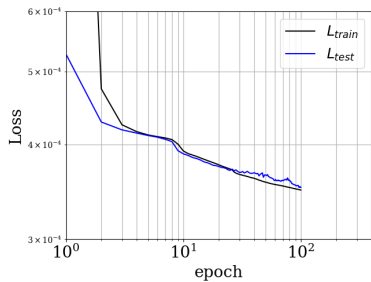
$$\arg \min_{\theta} \sum_{x_i, y_i \in \mathcal{d}} \frac{(y_i - \mu(\mathbf{x}_i))^2}{2\sigma(\mathbf{x}_i)} + \log(\sigma(\mathbf{x}_i)) + C$$

# Training a CNN-1d-SAL on the periodic hill $Re_b = 10,595$



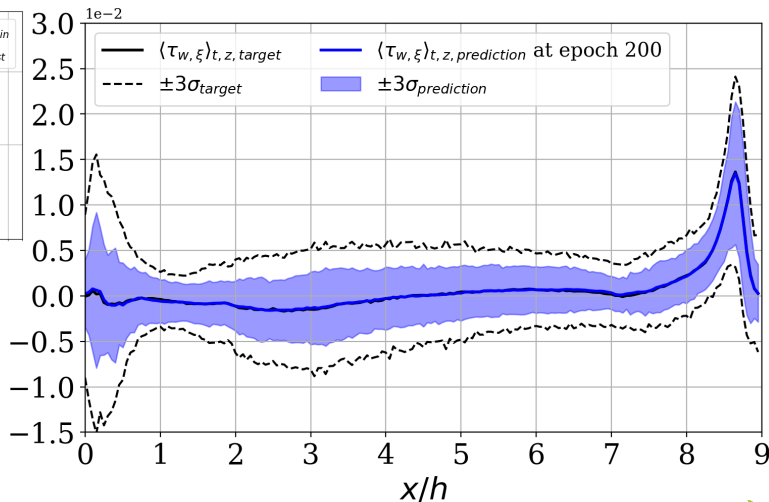
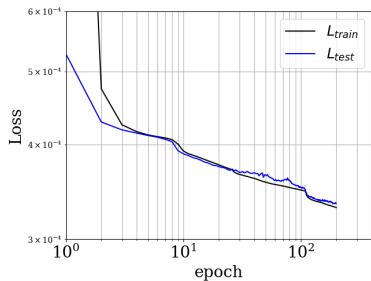
**#Parameters:** 6,440  
**Learning rate:** 0.001  
**Batch size:** 1024  
**Database size:** 2,736,000  
**Training time:** 5h13min  
**#Epoch:** 400

# Training a CNN-1d-SAL on the periodic hill $Re_b = 10,595$



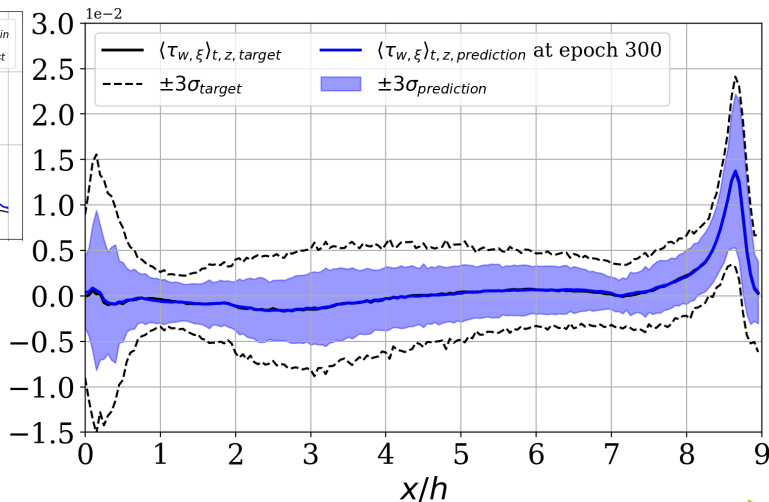
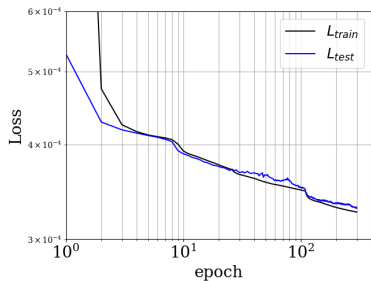
**#Parameters:** 6,440  
**Learning rate:** 0.001  
**Batch size:** 1024  
**Database size:** 2,736,000  
**Training time:** 5h13min  
**#Epoch:** 400

# Training a CNN-1d-SAL on the periodic hill $Re_b = 10,595$



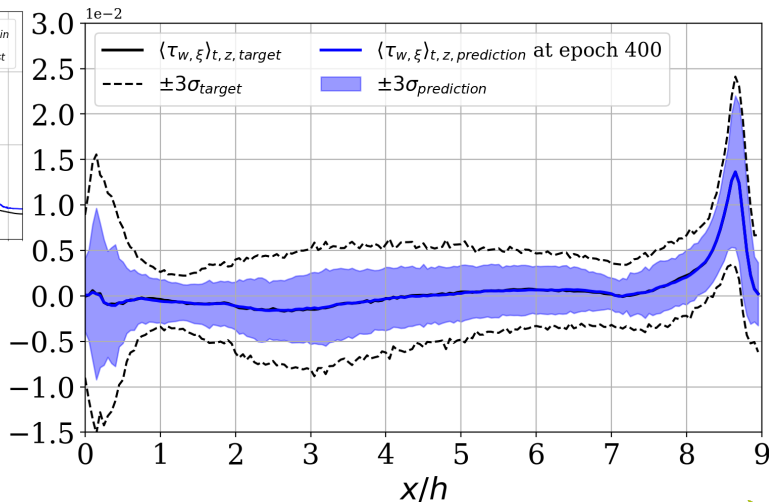
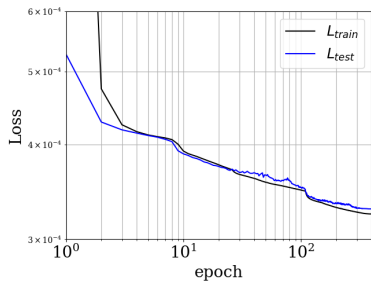
**#Parameters:** 6,440  
**Learning rate:** 0.001  
**Batch size:** 1024  
**Database size:** 2,736,000  
**Training time:** 5h13min  
**#Epoch:** 400

# Training a CNN-1d-SAL on the periodic hill $Re_b = 10,595$



**#Parameters:** 6,440  
**Learning rate:** 0.001  
**Batch size:** 1024  
**Database size:** 2,736,000  
**Training time:** 5h13min  
**#Epoch:** 400

# Training a CNN-1d-SAL on the periodic hill $Re_b = 10,595$



**#Parameters:** 6,440  
**Learning rate:** 0.001  
**Batch size:** 1024  
**Database size:** 2,736,000  
**Training time:** 5h13min  
**#Epoch:** 400



# A priori validation on the periodic hill $Re_b = 10,595$

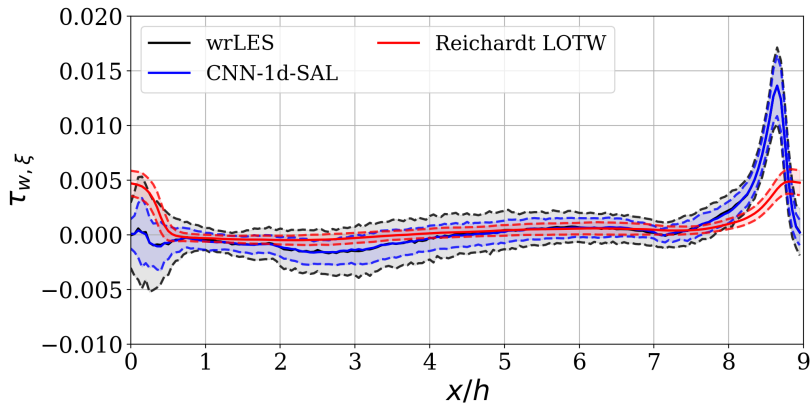
**Distribution** of the wall shear stress

**Instantaneous** wall-shear stress field

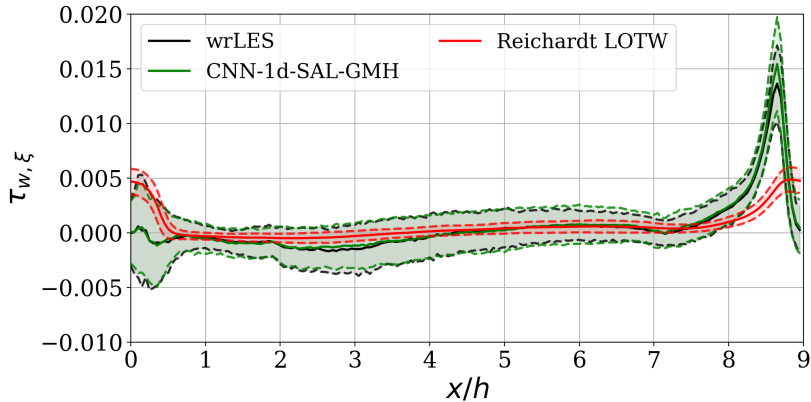
**Autocorrelations** of the predicted structures

Power **Spectrum** Density (PSD)

## Distribution of the wall shear stress

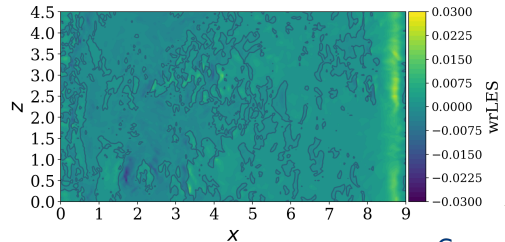
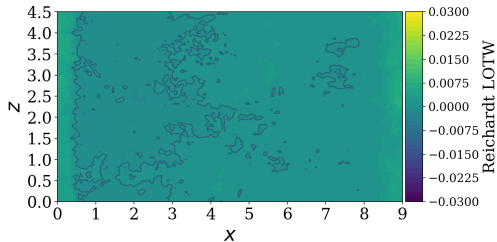
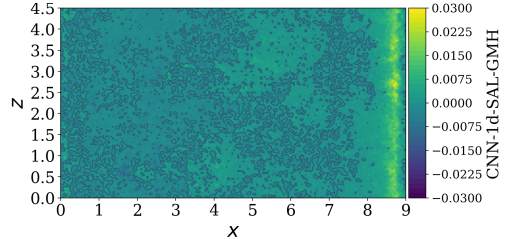
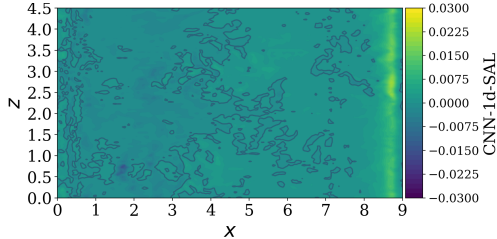


## Distribution of the wall shear stress

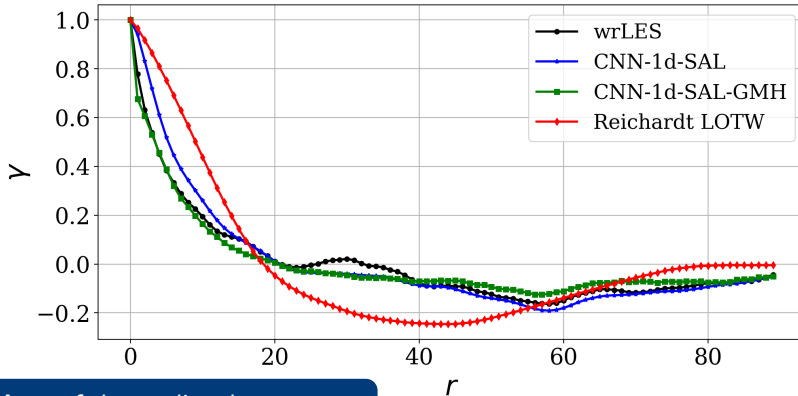


# A priori validation on the periodic hill $Re_b = 10,595$

## Instantaneous wall-shear stress field



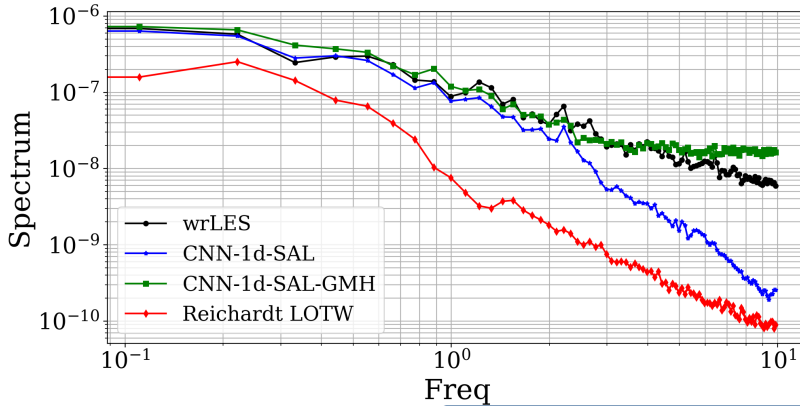
# A priori validation on the periodic hill $Re_b = 10,595$



## Autocorrelations of the predicted structures

Of  $\tau_{w,\xi}$  at a given time  $t$  computed in the  $\xi$ -direction and averaged in the  $z$ -direction.

# A priori validation on the periodic hill $Re_b = 10,595$

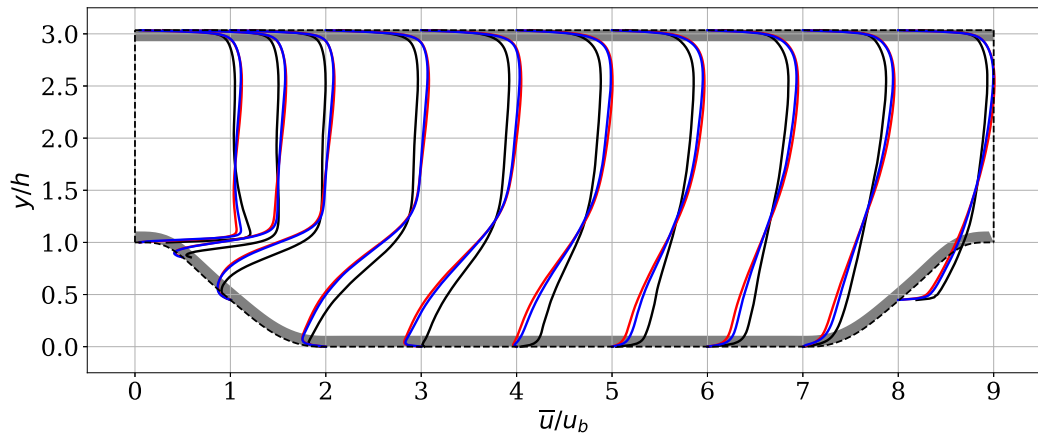


Power Density Spectrum (PDS)

Of  $\tau_{w,\xi}$  at a given time  $t$  computed in the  $\xi$ -direction and averaged in the  $z$ -direction.

# A posteriori validation on the CNN-1d-SAL for the periodic hill $Re_b = 10,595$

Velocity profiles averaged over 13.5 flow-through time:



**Remark:** The size of the recirculation bubble is underestimated and it impacts the whole domain.

# A posteriori validation on the CNN-1d-SAL for the periodic hill $Re_b = 10,595$

## How to correct the recirculation bubble location?

- Directional inconsistency [J. Bae *et al.*, 2022] between
  - the direction of the wall shear stress predicted by the network
  - the direction of the velocity measured at  $h_{wm}$



# A posteriori validation on the CNN-1d-SAL for the periodic hill $Re_b = 10,595$

## How to correct the recirculation bubble location?

- Directional inconsistency [J. Bae *et al.*, 2022] between
  - the direction of the wall shear stress predicted by the network
  - the direction of the velocity measured at  $h_{wm}$
- A quick fix in the code:

$$\boldsymbol{\tau}_w \cdot \boldsymbol{u} < 0 \Rightarrow \boldsymbol{\tau}_w = \mathbf{0}$$

# A posteriori validation on the CNN-1d-SAL for the periodic hill $Re_b = 10,595$

## How to correct the recirculation bubble location?

- Directional inconsistency [J. Bae *et al.*, 2022] between
  - the direction of the wall shear stress predicted by the network
  - the direction of the velocity measured at  $h_{wm}$

- A quick fix in the code:

$$\boldsymbol{\tau}_w \cdot \mathbf{u} < 0 \Rightarrow \boldsymbol{\tau}_w = \mathbf{0}$$

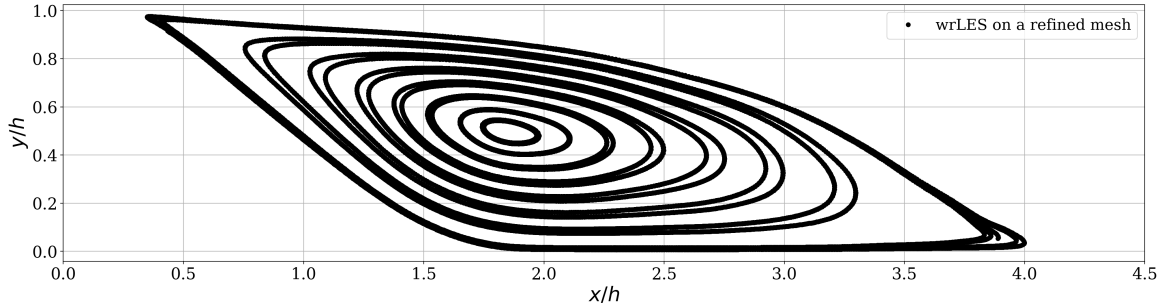
- Can also be added as an inequality constraint in the objective function while training the neural network as,

$$\mathcal{L} = \sum_{\mathbf{x}_i, \mathbf{y}_i \in \mathbf{d}} [(\tau_{\xi, i} - \hat{\tau}_{\xi, i})^2 + (\tau_{z, i} - \hat{\tau}_{z, i})^2] + \lambda \sum_{\mathbf{x}_i, \mathbf{y}_i \in \mathbf{d}} \text{ReLU}(-\boldsymbol{\tau}_i \cdot \mathbf{u}_i),$$

where  $\lambda$  is a certain hyper-parameter that penalizes more or less the directional inconsistency in the training dataset.

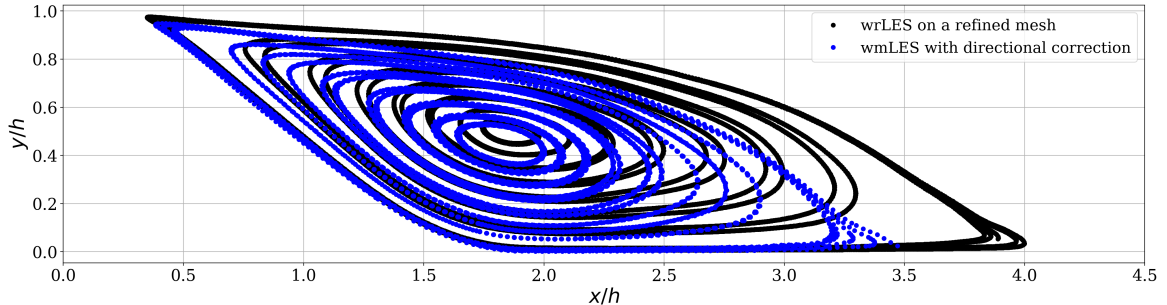
# A posteriori validation on the CNN-1d-SAL for the periodic hill $Re_b = 10,595$

Observation of the **streamlines** in the recirculation bubble using the quick fix:



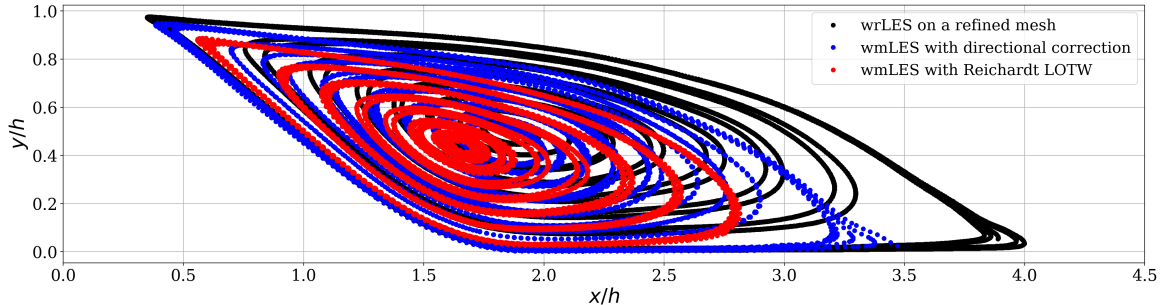
# A posteriori validation on the CNN-1d-SAL for the periodic hill $Re_b = 10,595$

Observation of the **streamlines** in the recirculation bubble using the quick fix:



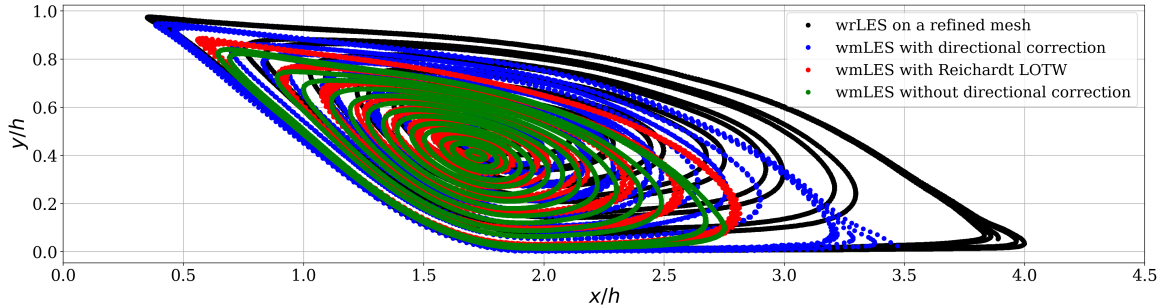
# A posteriori validation on the CNN-1d-SAL for the periodic hill $Re_b = 10,595$

Observation of the **streamlines** in the recirculation bubble using the quick fix:

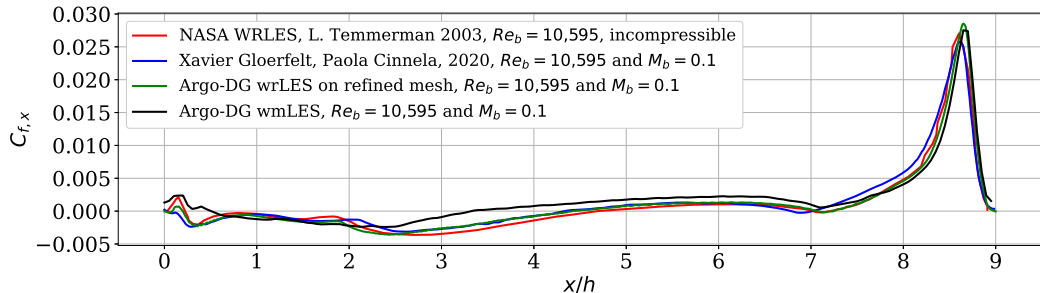


# A posteriori validation on the CNN-1d-SAL for the periodic hill $Re_b = 10,595$

Observation of the **streamlines** in the recirculation bubble using the quick fix:

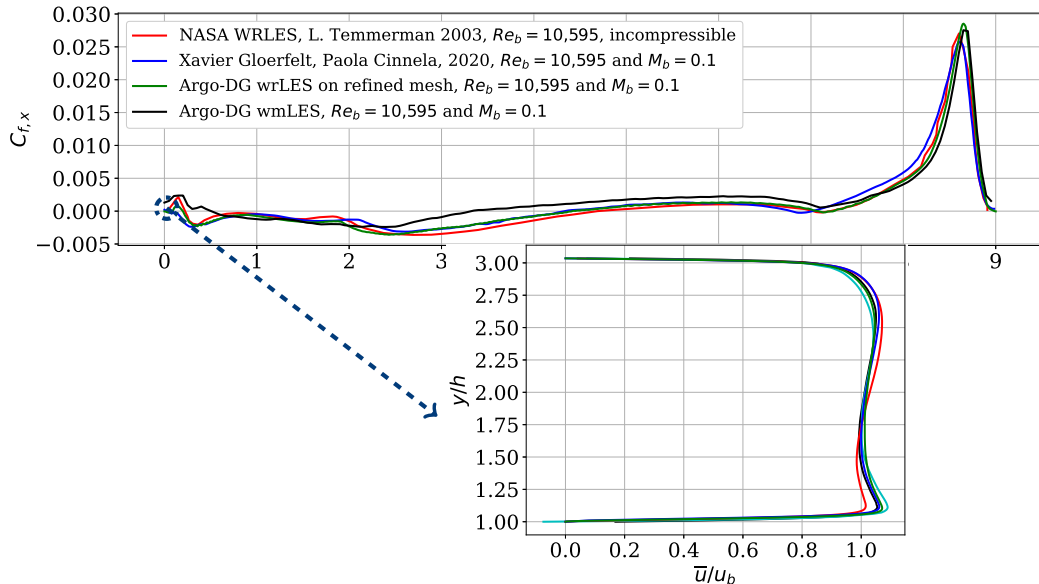


## A posteriori validation on the lower wall of the periodic hill $Re_b = 10,595$



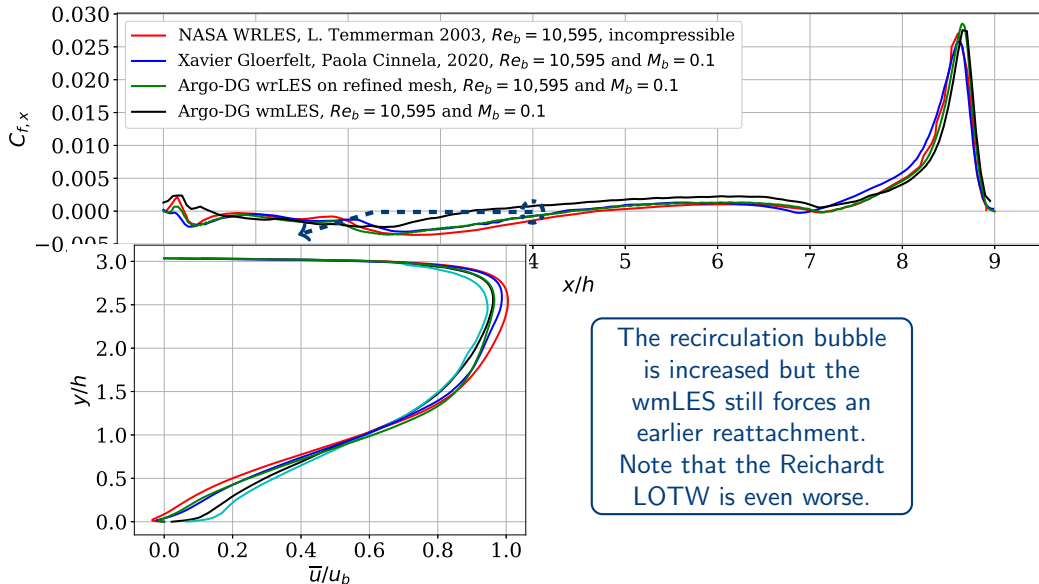
**Mean velocity profiles** at three  $x/h$  locations on the lower wall compared to the literature and a Reichardt LOTW (in cyan) computed with Argo-DG

# A posteriori validation on the lower wall of the periodic hill $Re_b = 10,595$



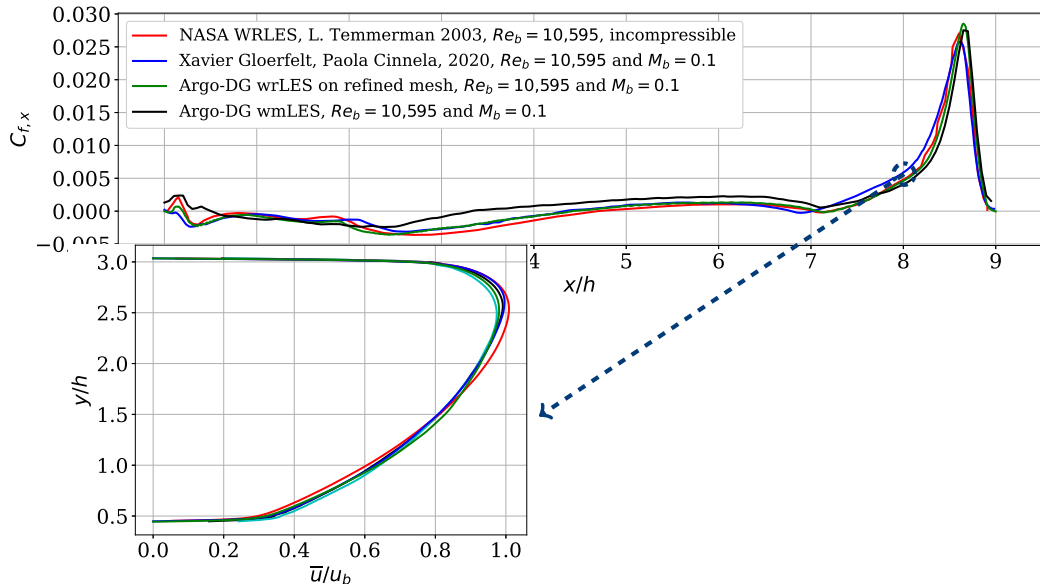


# A posteriori validation on the lower wall of the periodic hill $Re_b = 10,595$

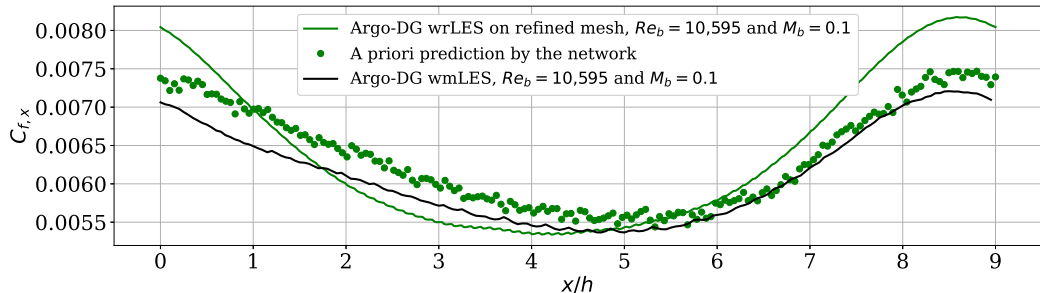


The recirculation bubble is increased but the wmLES still forces an earlier reattachment. Note that the Reichardt LOTW is even worse.

# A posteriori validation on the lower wall of the periodic hill $Re_b = 10,595$



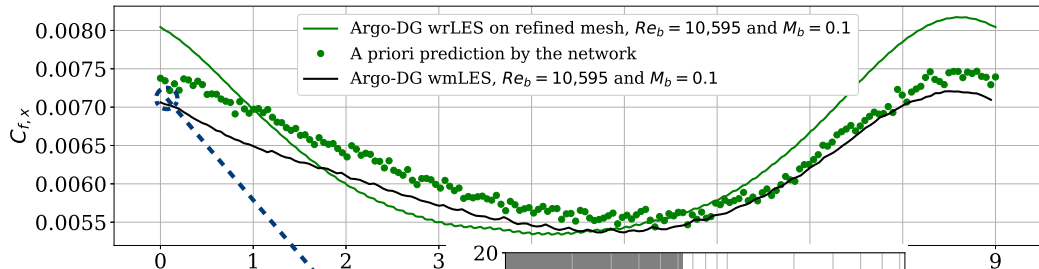
## A posteriori validation on the upper wall of the periodic hill $Re_b = 10,595$



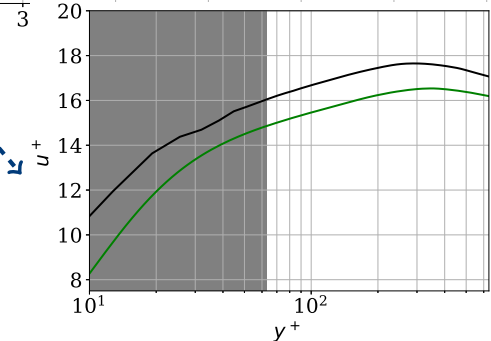
**Mean non-dimensional velocity profiles** at two  $x/h$  locations on the **upper wall** compared to the wrLES on a refined mesh.

**Remarks:** The wmLES friction coefficient is similar to the one *a priori* predicted by the neural network **but** the a priori one is far from the true value.

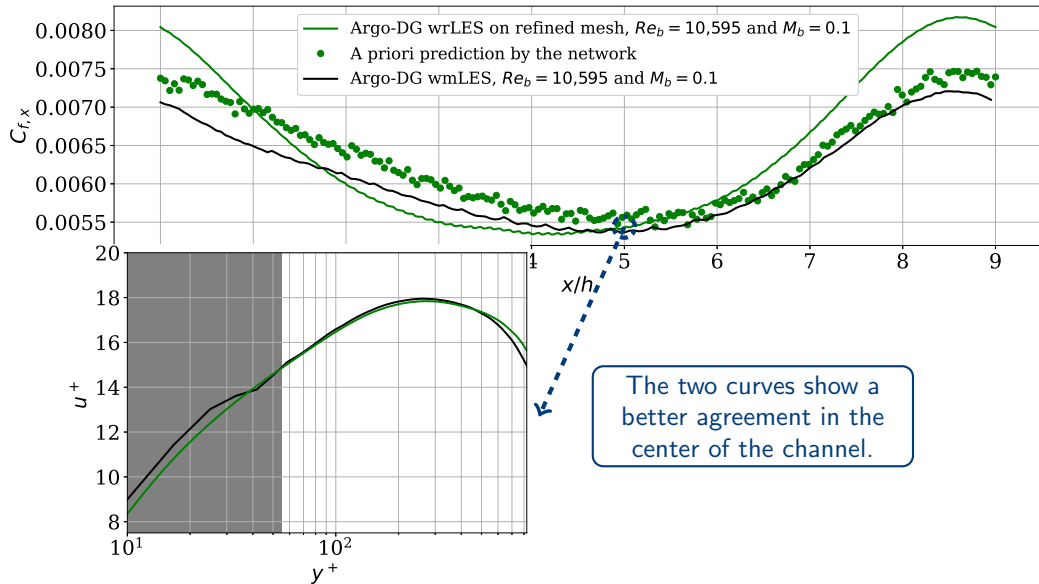
# A posteriori validation on the upper wall of the periodic hill $Re_b = 10,595$



The relative error at  $x/h = 0$  is 11% and hence we observe a discrepancy w.r.t. the wrLES non-dimensional profiles.



# A posteriori validation on the upper wall of the periodic hill $Re_b = 10,595$



- The *a posteriori* validation on the periodic hill, initially, gives:
  - a **wrong** recirculation bubble size;
  - a too **early** reacceleration of the flow;

which impacts the whole physics.

- Using the **directional correction** proposed earlier, the recirculation bubble size increases, but it is still smaller than the wrLES one.

- The *a posteriori* validation on the periodic hill, initially, gives:
  - a **wrong** recirculation bubble size;
  - a too **early** reacceleration of the flow;

which impacts the whole physics.

- Using the **directional correction** proposed earlier, the recirculation bubble size increases, but it is still smaller than the wrLES one.
- The non-dimensional velocity profiles on the upper wall **need to be corrected** (i.e., the relative error of 11% approximately) with a better neural network.
  - hard to predict with the neural network;
  - need to have more information in the input stencil (e.g., velocity gradient);
  - need to change the normalization (i.e., use the friction velocity).



The present research benefited from computational resources made available on the **Tier-1 supercomputer** of the Fédération Wallonie-Bruxelles, infrastructure funded by the Walloon Region under the grant agreement n°1117545. We would also like to gratefully acknowledge **SafranTech's** funding of Mrs. Boxho's thesis.